IOVS Papers in Press. Published on December 3, 2009 as Manuscript iovs.09-4650

Whirlin associates with the $Ca_v1.3$ (α_{1D}) channels in photoreceptors, defining a novel member of the Usher protein network

Ferry F.J. Kersten[1-5], Erwin van Wijk[1,2,4,5], Jeroen van Reeuwijk[1,4], Bert van der Zwaag[6], Tina Märker[7], Theo A. Peters[2,4,5], Nicholas Katsanis[8], Uwe Wolfrum[7], Jan E.E. Keunen[3], Ronald Roepman[1,4,ψ] and Hannie Kremer[2,4,5,ψ,#]

From the [1]Department of Human Genetics, [2]Department of Otorhinolaryngology, Head and Neck Surgery, and [3]Department of Ophthalmology, Radboud University Nijmegen Medical Centre, Nijmegen, The Netherlands, [4]Nijmegen Centre for Molecular Life Sciences, and [5]Donders Institute for Brain, Cognition and Behaviour, Radboud University Nijmegen, Nijmegen, The Netherlands, [6]Department of Neuroscience and Pharmacology, Rudolf Magnus Institute of Neuroscience, University Medical Centre Utrecht, Utrecht, The Netherlands, [7]Department of Cell and Matrix Biology, Institute of Zoology, Johannes Gutenberg University of Mainz, Mainz, Germany, [8]McKusick-Nathans Institute of Genetic Medicine and Departments of Ophthalmology and Molecular Biology and Genetics, Johns Hopkins University, Baltimore, Maryland, 210205 USA. [ψ]These authors contributed equally to this work.

[#]To whom correspondence should be addressed at: Department of Otorhinolaryngology, Radboud University Medical Centre, Internal Postal Code 377, PO Box 9101, 6500 HB Nijmegen, The Netherlands. Tel: +31 243610487; Fax: +31 243668752; Email: h.kremer@antrg.umcn.nl

This research was supported by the Radboud University Nijmegen Medical Centre, Nijmegen, The Netherlands, The British Retinitis Pigmentosa Society (GR552), and by the Heinsius Houbolt Foundation.

Title characters: 121

Abstract 250 words: 240

Text words: 4323

PURPOSE. Usher syndrome is the most common form of hereditary deaf-blindness. It is both clinically and genetically heterogeneous. The USH2D protein whirlin interacts via its PDZ domains with other Usher-associated proteins containing a C-terminal type I PDZ binding motif. These proteins co-localize with whirlin at the region of the connecting cilium and at the synapse of photoreceptor cells. This study was undertaken to identify novel, Usher syndrome-associated, interacting partners of whirlin and thereby obtain more insights into the function of whirlin.

METHODS. The database of ciliary proteins was searched for proteins that are present in both retina and inner ear and contain a PDZ-binding motif. Interactions with whirlin were evaluated by yeast two-hybrid analyses, and validated by glutathione *S*-transferase pull-down assays, co-immunoprecipitations and co-localization in the retina with immunofluorescence and immunoelectron microscopy.

RESULTS. The L-type calcium channel subunit $Ca_v1.3$ (α_{1D}) specifically interacts with whirlin. In adult photoreceptors, $Ca_v1.3$ (α_{1D}) and whirlin co-localize in the region of the connecting cilium and at the synapse. During murine embryonic development, the expression patterns of the *Whrn* and *Cacna1d* genes show significant overlap and include expression in the eye, the inner ear and the central nervous system.

CONCLUSIONS. Our findings indicate that $Ca_v1.3$ (α_{1D}) is connected to the Usher protein network. We hypothesize that in the retina whirlin scaffolds $Ca_v1.3$ (α_{1D}) and therefore contributes to the organization of calcium channels in the photoreceptor cells, where both proteins may be involved in membrane fusions.

Usher syndrome is the most common form of hereditary deaf-blindness in man and has an autosomal recessive pattern of inheritance. Three clinical types, types USH1-USH3, are distinguished based on the progression and severity of the hearing loss and the presence or absence of vestibular dysfunction, with visual loss due to retinitis pigmentosa (RP) in all three types.[1] To date, the affected genes have been identified for nine out of the twelve described Usher loci.[2-10] Besides being causative for Usher syndrome, mutations in the Usher genes *MYO7A, USH1C, CDH23, PCDH15* and *DFNB31* are also associated with non-syndromic hearing loss.[2, 6-10] In addition, mutations in the *USH2A* gene can lead to non-syndromic autosomal recessive RP.[2, 8, 11, 12] All USH1 and USH2 proteins are integrated in an Usher protein network in both the inner ear and the retina with a central scaffolding role for the proteins whirlin and harmonin.[6, 13-15] These proteins contain multiple PDZ domains, homologous to domains identified in postsynaptic density protein 95 (PSD-95), disc large (Dlg) and zonula occludens-1 (ZO-1), that link them to the intracellular moieties of transmembrane Usher proteins with a C-terminal PDZ-binding motif (PBM). The USH1 and USH2 proteins are prominently located in the ciliary transition zone (connecting cilium) and periciliary region of the photoreceptor cells, rendering Usher syndrome a ciliopathy. In addition, most of the proteins localize to the synapse of photoreceptor cells.[6-8, 14-16] At these specific sites, the Usher proteins are suggested to function in protein transport, structural support and organization of ion channels.[6, 8, 14, 17, 18]

To identify novel members of the Usher protein complex and thereby obtain more clues on the function of whirlin and harmonin, we employed a bioinformatic approach. This approach revealed the L-type calcium channel pore forming subunit $Ca_v1.3$ (α_{1D}) as a potential new member of the Usher protein complex. It is a transmembrane protein which is predicted to contain four transmembrane and four ion transport domains.[20] $Ca_v1.3$ (α_{1D})-deficient mice are deaf due to the complete absence of L-type currents in cochlear inner hair cells and both the inner and outer hair cells degenerate. The mice do not show any signs of vestibular dysfunction or retinal degeneration.[21] The zebrafish $Ca_v1.3a$ (α_{1D}) mutant does exhibit, besides hearing loss, a vestibular ("circling") phenotype, but no retinal degeneration has been described although the latter might be explained by the presence of a second copy of the gene which is differentially expressed in the retina.[22]

Here we describe the identification of a specific PDZ – PBM based interaction between whirlin and $Ca_v1.3$ (α_{1D}) and their co-localization in different layers of the retina including the outer limiting membrane (OLM), the outer plexiform layer (OPL) and in the region of the connecting cilium. We

suggest that in the retina, the interaction of whirlin with $Ca_v1.3$ (α_{1D}) contributes to the organization of voltage-gated L-type calcium channels**.**

MATERIALS AND METHODS

Bioinformatics

Swiss-Prot protein sequences were downloaded from UniProt (www.uniprot.org) in FASTA format and proteins matching the C-terminal class I PDZ binding motif (PBM; [ST].[VIL]$) (http://elm.eu.org/elmPages/LIG_PDZ_1.html) where extracted. The resulting dataset was filtered for proteins associated with ciliary function, using the Ciliary Proteome database v3.0 (www.ciliaproteome.org), study selection: all except for Liu et al. 2007, database type: all; cutoff *E*-value: 30. Subsequently, a filter for proteins that are encoded by genes expressed in eye or ear (www.ncbi.nlm.nih.gov/UniGene/) was applied. A final selection of candidate Usher proteins was made by selecting for homologs of mouse mutant proteins that are associated with vision/eye (MP:0005391) or hearing/vestibular/ear phenotype (MP:0005377) as contained in the Mouse Genome Informatics database (www.informatics.jax.org).

Animals

Wistar rats and C57BL6 JOlaHsD mice (Harlan, The Netherlands) used in this study were housed in standard cages and received water and food *ad libitum*. All experiments were conducted according to the ARVO Statement for the Use of Animals in Ophthalmic and Vision Research and international and institutional guidelines.

Cloning

Human Marathon brain cDNA (Clontech, CA) was used as a template to amplify the cDNA encoding part of the C-terminal intracellular domain of CACNA1D (amino acids (aa) 1938-2181). The aa numbers are according to the following GenBank entries: $Ca_v1.3$ (α_{1D}) NP_000711, whirlin NP_056219, harmonin NP_710142, Plk1 NP_005021. All constructs were generated using the Gateway cloning technology (Invitrogen, CA), according to the manufacturer's instructions.

Yeast Two-Hybrid Analysis

To test whether there is an interaction between $Ca_v1.3$ (α_{1D}) and whirlin, a Gal4-based yeast two-hybrid system (HybriZAP, Stratagene) was used according to methods previously described.[15, 23]

Antibodies

The antibodies against whirlin and centrins were previously described.[14, 15, 24] Anti-HA and anti-$Ca_v1.3$ were derived from Sigma (Germany). Anti-GFP (Roche, Germany) was used to detect eCFP tagged proteins. As secondary antibodies goat-anti-guinea pig Alexa 488, goat-anti-rat Alexa 568, IRDye800 goat-anti-guinea pig IgG, and IRDye800 goat-anti-mouse were used (all from Molecular Probes-Invitrogen, Carlsbad, CA).

GST Pull-Down

The GST-fusion proteins were produced by transforming E.coli BL21-DE3 with plasmids pDEST15-whirlin PDZ1 (aa 138-233), PDZ2 (aa 279-360), PDZ1+2 (aa 138-360), PDZ3 (aa 819-907), pDEST15-$Ca_v1.3$ (aa 1938-2181) or pDEST15-$Ca_v1.3\Delta$PBM (aa 1938-2175) according to methods previously described.[15] HA-tagged whirlin full length (aa 1-907), eCFP-$Ca_v1.3$ (aa 1938-2181) and eCFP-$Ca_v1.3\Delta$PBM (aa 1938-2175) were produced by transfecting COS-1 cells with pcDNA3-HA-Whirlin fl, pDEST501-$Ca_v1.3$ and pDEST501-$Ca_v1.3\Delta$PBM respectively using Effectene transfection reagent (QIAGEN, Germany) according the manufacturer's instruction. The follow-up of the experiment was previously described.[15]

Co-Immunoprecipitation in COS-1 Cells

Full length eCFP-tagged whirlin (aa 1-907) was expressed by using the expression vector pDest501. HA-tagged $Ca_v1.3$ (aa 1938-2181) and Plk1 (aa 1-603) were expressed by using the pcDNA3-HA/Dest expression vector. COS-1 cells were transfected by using Effectene transfection reagent (QIAGEN, Germany) according to the manufacturer's instruction. Twenty-four hours after transfection cells were washed with phosphate-buffered saline (PBS) and subsequently lysed on ice in IP lysis buffer.[15] eCFP-tagged whirlin was immunoprecipitated from cleared lysates overnight at 4 °C by using the anti-whirlin antibody.[15] HA-tagged $Ca_v1.3$ and Plk1 were immunoprecipitated by using anti-HA monoclonal antibody (Sigma, Germany) and protein A/G PLUS-Sepharose beads (Santa Cruz Biotechnology). The

protein complexes were washed four times with IP lysis buffer and subsequently analyzed on Western blots using the Odyssey Infrared Imaging System (LI-COR).

Immunohistochemistry in Rat Retina

Unfixed eyes of 20-day-old (P20) Wistar rats were isolated and frozen in melting isopentane. Seven µm cryosections were treated and immunolabeled as described previously.[15]

Digoxigenin Labelling of cRNA *In Situ* Hybridization Probes

A probe corresponding to nucleotides 556-1673 (GenBank NM_001083616), which recognizes mouse *Cacna1d* transcripts was generated from mouse retina Marathon cDNA (Clontech) using 5'-gcgaacgaggcaaactatg -3' as a forward primer and 5'- ccaaggatgatcagactaac -3' as a reversed primer. The labeling was performed as previously described.[15]

RNA *In Situ* Hybridization

C57Bl6 Jlco mouse embryos were collected at various embryonic stages (E12.5 to E18.5), as well as postnatal day 7 (P7) and P90 mouse eyes. RNA *in situ* hybridization was performed as previously described.[15] To increase structural detail, a number of slides were incubated in Nuclear Fast Red (Sigma) for 10 seconds before embedding in Entellan rapid mounting media (ProSciTech). Images were recorded on a Zeiss Axioskop2 plus microscope with a Sony power HAD DXC-950P 3CCD color video camera.

Pre-Embedding Immunoelectron Microscopy

Vibratome sections of mouse retina were stained by a 100 times diluted antibody against $Ca_v1.3$ (α_{1D}) and visualized by a secondary antibody (Vectastain ABC-Kit, Vector, England). After fixation with 0.5% OsO_4 specimens were embedded in araldite and ultrathin sections were analyzed with a FEI Tecnai 12 transmission electron microscope. The procedure was described in detail previously.[17]

RESULTS

Identification of Candidate Members of the Usher Proteome Complex

To obtain more clues on the function of whirlin and harmonin, we used a bioinformatic approach to identify novel members of the Usher protein complex. We developed a script to select for human

proteins from the Swiss-Prot database (www.uniprot.org) that match the class I PBM, as many of the interactions in the Usher protein network are PDZ – PBM based.[6, 15] Out of the resulting 955 proteins, 147 are present in the ciliary proteome database.[25] As our candidate Usher genes should be expressed in the eye or inner ear, a filter for expression in eye or ear (www.ncbi.nlm.nih.gov/UniGene/) yielded 117 genes. We then used the Mouse Genome Informatics (MGI) database (www.informatics.jax.org) to restrict our selection of candidate Usher genes to genes which are associated with vision/eye (MP:0005391) or hearing/vestibular/ear phenotypes (MP:0005377) in mice. This query yielded eighteen genes including the three of the known Usher genes *CDH23*, *PCDH15* and *USH2A*, which validates our approach. Out of these eighteen genes, we selected the gene encoding the L-type calcium channel pore forming subunit $Ca_v1.3$ (α_{1D}) as a very promising candidate Usher gene for further analysis, since the phenotype of early hair cell degeneration in the cognate mouse mutant[21] is most similar to the phenotypes of the known Usher mouse mutants.[Reviewed in 26]

$Ca_v1.3$ (α_{1D}) and Whirlin Interact Directly

A yeast two-hybrid assay was used to assess whether the PDZ domains of whirlin and harmonin associate with part (aa 1938-2181) of the intracellular C-terminal tail of $Ca_v1.3$ (α_{1D}), which contains a class I PBM (aa 2178-2181). We identified an interaction between the cytoplasmic region of $Ca_v1.3$ (α_{1D}) and the N-terminal two PDZ domains of whirlin (Fig. 1A). Weak associations of $Ca_v1.3$ (α_{1D}) with PDZ1 and PDZ3 of harmonin were suggested by limited growth of the yeast colonies. No interaction between the $Ca_v1.3$ (α_{1D}) C-terminus and whirlin PDZ3 or harmonin PDZ2 could be detected (Fig. 1A). The association of whirlin and $Ca_v1.3$ (α_{1D}) was confirmed by using a glutathione *S*-transferase (GST) pull-down assay. Full-length HA-tagged whirlin was efficiently pulled down from COS-1 cell lysates by the GST-fused C-terminal part of $Ca_v1.3$ (α_{1D}), but not by GST alone (Fig. 1B). Deletion of the predicted C-terminal class I PBM in $Ca_v1.3$ (α_{1D}) disrupts the binding, indicating that this interaction is indeed based on a PDZ – PBM association (Fig. 1B).

To confirm that specifically the PDZ domains 1 and 2 of whirlin are involved in this interaction, we expressed the domains separately as GST fusion proteins to pull down the enhanced cyan fluorescent protein (eCFP)-tagged cytoplasmic tail of $Ca_v1.3$ (α_{1D}). As shown in Fig. 1C, whirlin PDZ1, PDZ2 and a

peptide containing both PDZ domains are able to bind to the C-terminal part of $Ca_v1.3$ (α_{1D}), but not PDZ3 or GST alone.

As a further validation of the interaction *in vivo*, a co-immunoprecipitation assay from COS-1 cells was performed, which showed that full length eCFP-tagged whirlin specifically co-immunoprecipitates with the HA-tagged C-terminus of $Ca_v1.3$ (α_{1D}) but not with the unrelated HA-tagged protein Plk1 (Fig. 1D). In contrast, HA-tagged harmonin was not pulled down from COS-1 cell lysates with the GST-fused C-terminal part of $Ca_v1.3$ (α_{1D}) (Fig. 1E). Therefore the interaction between harmonin and $Ca_v1.3$ (α_{1D}) was not further investigated.

$Ca_v1.3$ (α_{1D}) and Whirlin Co-localize in the Retina

To investigate whether $Ca_v1.3$ (α_{1D}) and whirlin indeed co-localize in the retina, we co-immunostained retinal cryosections with antibodies against whirlin (green) (Fig. 2A) and $Ca_v1.3$ (α_{1D}) (red) (Fig. 2B). This revealed high expression and co-localization of these proteins (Fig. 2C) at the region of the connecting cilium, the OLM and the OPL. Immunostaining of $Ca_v1.3$ (α_{1D}) was also observed at the inner plexiform layer (IPL) (Fig. 2B, C). Double immunostaining of $Ca_v1.3$ (α_{1D}) and centrins, markers for the accessory centriole, basal body and connecting cilium,[24] further confirmed the localization of $Ca_v1.3$ (α_{1D}) in this region since a (partial) co-localization was observed (Fig. 2D-F).

Recently, the subcellular localization of whirlin in the mouse photoreceptor was determined using immunoelectron microscopy.[6, 17] Here, we present this for $Ca_v1.3$ (α_{1D}). Pre-embedding labelling with an antibody directed against $Ca_v1.3$ (α_{1D}) revealed its localization in the collar-like extension of the apical inner segment (Fig. 3A-B), at the basal body complex (Fig. 3B-C), in the connecting cilium (Fig. 3B-D), in the basal region of the outer segments (Fig. 3A-C) and at the synapse (Fig. 3E-F) of mouse photoreceptor cells. As whirlin was also detected at these exact sub-cellular sites, with the exception of the outer segments and the synapse,[6, 17] these results confirm the co-localization of $Ca_v1.3$ (α_{1D}) and whirlin.

***Cacna1d* Expression During Murine Development**

The expression of *Cacna1d* in development was assessed by RNA *in situ* hybridization using mouse embryos of gestational days 12.5-18.5 (E12.5-E18.5) and eyes of mice at postnatal days 7 and 90 (P7 and P90). *Cacna1d* was widely expressed during murine embryonic development. From E12.5 to

E16.5 expression was observed in the eye, inner ear, thalamus, neopallial cortex, midbrain, choroid plexus of the fourth ventricle, spinal cord, jaw, olfactory bulb, olfactory epithelium, lung, tongue, trigeminal (V) ganglion, duodenum, umbilical cord, venous heart region, kidney, adrenal gland and the stomach wall (Fig. 4A, and data not shown). At E18.5, the expression became more restricted and was detected in the lung, kidney, spinal cord, olfactory epithelium and intense staining was observed in the brain, inner ear (data not shown) and eye (Fig. 4E). In the developing retina, *Cacna1d* was transcribed from E12.5 onwards (Fig. 4B-H). At E12.5, there was a strong signal in the complete neuroblastic layer (Fig. 4B). The signal at E14.5 was comparable with that at E12.5, but no staining was detected at the outermost cells. At E16.5, expression was detected in the inner neuroblastic layer of the retina, with the highest signal intensity in the area around the developing lens (Fig. 4D). At E18.5 the *Cacna1d* expression could be clearly distinguished in a subset of the ganglion cells, the inner nuclear layer (INL) and low intensity staining was present in the neuroepithelium surrounding these layers (Fig. 4E). In juvenile postnatal day 7 (P7) and day 90 (P90) eyes, *Cacna1d* transcripts were detected in the INL, the outer nuclear layer (ONL) and in the inner segments. A high intensity signal, suggestive of a high level of *Cacna1d* expression, was seen in a subset of the ganglion cells and in INL (Fig. 4F-H). In the developing inner ear, distinct expression was observed from E14.5 onwards, which became more pronounced at E16.5 (Fig. 4I). At higher magnification we show the expression of *Cacna1d* in the vestibular system and cochlea of the E16.5 inner ear (Fig. 4J). To obtain more structural detail for the inner ear, a number of sections of an E16.5 embryo were counterstained with Nuclear Fast Red. This revealed that *Cacna1d* expression was situated in the inner hair cells (IHC) of the cochlea and in spiral ganglion cells (Fig. 4L-M). Also expression in the developing sensory cells of the macula of the utricle and the cristae ampullaris of the semicircular canals was detected (Fig. 4N-O). Hybridizations with a sense cRNA probe revealed no signals, indicating the specificity of the antisense cRNA probe used in these experiments (Fig. 4K).

DISCUSSION

In this study, we demonstrate that the C-terminus of the calcium channel subunit $Ca_v1.3$ (α_{1D}) interacts with PDZ1 and PDZ2 of whirlin and that these proteins co-localize at distinct sites in photoreceptor cells. A functional calcium channel is a heteromultimeric protein complex, composed of a pore-forming

α_1 subunit, like $Ca_v1.3$ (α_{1D}) and the auxiliary subunits β, γ, and $\alpha_2\delta$. Ten α_1-subunit pore-forming isoforms (α_{1a} - α_{1I} and α_{1S}) of voltage-activated calcium channels are described.[27] The α_1 subunit imparts most of the conductive properties of the channel, whereas the accessory subunits modulate calcium currents and channel activation/inactivation kinetics.[28-30]

$Ca_v1.3$ (α_{1D}), encoded by the *CACNA1D* gene, is the most abundant isoform in hair cells and fulfills distinct physiological roles in the inner ear.[21, 31] In the retina of mouse, rat and zebrafish, $Ca_v1.3$ (α_{1D}) mRNA has been observed in the ONL, the INL, and in the ganglion cell layer (GCL).[22, 32-34] At the protein level, $Ca_v1.3$ (α_{1D}) has been detected in the Müller cells, the OPL and photoreceptor cell bodies of the rat retina.[34] In the salamander retina immunoreactivity is observed in the GCL, Müller cells, the IPL, the OPL, and in the photoreceptor inner segment.[35, 36]

During development, the murine *Cacna1d* gene is widely expressed, *e.g.* in the eye, the inner ear and in the CNS. Interestingly, *Whrn* expression was also detected in these tissues.[15] We and others have shown that whirlin is connected to the dynamic Usher protein interactome and we suggested that whirlin mediates multiple biological processes in the inner ear and the retina.[6, 15] Our findings indicate that through whirlin, $Ca_v1.3$ (α_{1D}), a voltage gated calcium channel subunit, is connected to the Usher protein network, underlining the molecular diversity of this interactome.

Cacna1d Expression During Murine Development

At early embryonic stages (E12.5-E14.5) *Cacna1d* expression was detected in the eye, the inner ear, the midbrain, spinal cord, tongue, lung, choroid plexus of the fourth ventricle and kidney, in which also *Whrn* RNA was shown to be present.[15] This overlap in expression may indicate a function of both proteins in the same complex already at these early embryonic stages in several tissues. In the developing inner ear *Cacna1d* expression was observed in the cochlear IHCs, the spiral ganglion cells and the sensory cells of the vestibular part. Also, *Whrn* is expressed in these cells, although in the sensory epithelium of the cochlea only detectable from E18.5 onwards.[15] In a recent study, RNA *in situ* hybridization was performed on whole-mount preparations of mature mouse organs of Corti, and *Cacna1d* mRNA was detected in both IHCs and outer hair cells (OHC), but mainly in the OHCs.[37] We were only able to show *Cacna1d* expression in the IHCs. This discrepancy may be explained by the difference in age of the animals, embryonic stages in our study versus P19 in the study of Knirsch *et al.*.[37]

At early developmental stages of the retina, both *Cacna1d* (present data) and *Whrn* (previously described by van Wijk *et* al.[15]) are expressed, although *Whrn* transcripts are mainly present in the innermost layers, whereas *Cacna1d* transcripts are detected in the entire developing retina. From E16.5 onwards, the retinal expression patterns of *Cacna1d* and *Whrn* have a higher similarity. The *Cacna1d* expression in the adult mouse retina is observed in all three nuclear layers (GCL, INL, ONL) which is consistent with the findings in a previous study.[33] The difference in relative signal strength between the study of Xiao *et al.*[33] and the data we present may be due to a difference in antibody concentration and colorimetric reaction time. In postnatal stages of retinal development and in adult retina, *Cacna1d* expression is most prominent in the INL whereas *Whrn* expression is highest in the ONL. The overlap in *Cacna1d* and *Whrn* expression at several stages of mouse development and in several organs, although at an apparently different quantitative distribution, together with the interaction at the protein level indicates that $Ca_v1.3$ (α_{1D}) and whirlin serve in the same processes of neuronal differentiation.

$Ca_v1.3$ (α_{1D}) Localization and Function in the Photoreceptor

In mature photoreceptor cells, $Ca_v1.3$ (α_{1D}) and whirlin co-localize at regions where also Usher syndrome-associated proteins such as USH2A, SANS and GPR98 (VLRG1) co-localize with whirlin.[14, 15, 17] We previously suggested that whirlin may contribute to the organization of ion channels in the pre- and/or postsynaptic membranes of hair cells and photoreceptor cells.[6, 14, 15] Our present data indicate that $Ca_v1.3$ (α_{1D}) is one of these ion channels at the OPL of the photoreceptor. In contrast to $Ca_v1.3$ (α_{1D}), whirlin was not observed at the IPL by immunohistochemistry which indicates that whirlin does not play a role in $Ca_v1.3$ (α_{1D}) organization in the synapses of this layer. Expression of whirlin, synonymously named CIP98, was not only detected in the synaptic region of the photoreceptor cells, but also in the synaptic regions of the cochlear sensory cells[15] and possibly in neurons in the brain. Whirlin interacts with calmodulin-dependent serine kinase (CASK) and both proteins are co-immunoprecipitated from brain extracts. The whirlin-CASK complex has been suggested to play a role in trafficking of synaptic vesicles for transmission.[38] Interestingly, CASK is also detected at the OPL of the retina[39] and therefore whirlin might serve as an adaptor protein linking CASK and $Ca_v1.3$ (α_{1D}) in the synaptic regions of the retinal sensory cells. The complex might participate in the regulation of neurotransmission via the organization of $Ca_v1.3$ (α_{1D}) channels in the photoreceptor cell synapses.

Also, in the inner ear, $Ca_v1.3$ (α_{1D}) channels are involved in the regulation of exocytosis of synaptic vesicles in IHCs and probably also in OHCs.[37, 41-43] Although whirlin was not detected in the synaptic region of IHCs, it was found to be present in the synaptic region of OHCs[15] and therefore the whirlin-$Ca_v1.3$ (α_{1D}) interaction might play a role in synaptic transmission in these cells as well. However, in order to confirm this hypothesis, the localization of whirlin and its co-localization with $Ca_v1.3$ (α_{1D}) in the synaptic region of OHCs should be studied in more detail.

The role of $Ca_v1.3$ (α_{1D}) and its possible interaction with whirlin at the basal body and in the connecting cilium remains elusive. It is thought that the basal body functions in the organization of transport of cytoplasmic and transmembrane proteins into and through the connecting cilium. Therefore, the presence of whirlin and $Ca_v1.3$ (α_{1D}) in the basal body might be explained by the fact that they are transported from there into the connecting cilium where both proteins have been detected. In the connecting cilium, the whirlin-$Ca_v1.3$ (α_{1D}) interaction may function in the organization of the channels and thereby in the Ca^{2+} homeostasis in this region and the regulation of the Ca^{2+}-dependent interaction of centrins and the visual G-protein transducin.[24] The centrin-transducin interaction is thought to regulate the light dependent translocation of transducin through the connecting cilium.[24]

Recently, our group and others described the molecular and ultrastructural homology between the periciliary structures in mammalian and amphibian photoreceptor cells. In mammals the membrane domain of the apical inner segment collar corresponds to the periciliary ridge complex (PRC) of the amphibian photoreceptor.[17, 44] Besides providing structural support of the connecting cilium, this region is thought to function in docking trans-Golgi derived cargo vesicles containing proteins that are essential for outer segment formation and renewal and phototransduction.[6, 17, 45, 46] We previously identified whirlin as one of the major molecules of the PRC[17] and subsequently Mazelova et al. used an antibody against whirlin as a marker for the PRC,[47] demonstrating the association of the SNARE proteins syntaxin 3 and SNAP25 with this region.[47] Also, here the interaction of whirlin and $Ca_v1.3$ (α_{1D}) may have a role in the transport to or organization of the calcium channel at the plasma membrane. The role of the $Ca_v1.3$ (α_{1D}) channel at these subcellular sites might be the regulation of docking and fusion of cargo vesicles, involving SNARE proteins, through mediation of the Ca^{2+} concentration and $Ca_v1.3$ (α_{1D}) was shown to be in a complex with SNARE proteins.[48, 49] As is shown

for synaptic vesicle fusion and exocytosis, the increase in Ca^{2+} concentration via Ca^{2+} influx through voltage-gated calcium channels initiates these processes.[29, 50] Interestingly, $Ca_v1.3$ (α_{1D}) was also detected in the pericuticular region of hair cells in the inner ear.[43] and in this region also SNARE proteins were detected.[51] This region is thought to be the site of vesicular trafficking, endocytosis, exocytosis and membrane recycling for stereocilia repair[52] and therefore may have functional similarities to the periciliary region of photoreceptor cells.

We detected $Ca_v1.3$ (α_{1D}) also at the base of the outer segments. At this site the process of outer segment disc morphogenesis occurs. Rab and SNARE proteins, present in this region are suggested to contribute to this process by mediating membrane fusion of vesicles containing outer segment proteins.[53, 54] For vesicles loaded with rhodopsin the targeting and fusion was indicated to be regulated by the protein SARA through its direct interaction with rhodopsin, syntaxin 3 and PI3P.[53] The Ca^{2+}-dependence of the process of membrane fusion[55-57] as discussed in the previous paragraph, may explain the presence of $Ca_v1.3$ (α_{1D}) in this region.

CACNA1D in Disease

Voltage-gated L-type calcium channels contribute to retinal signal transmission.[58] Recently, it has been shown that a mutation in the *CACNA2D4* gene which encodes one of the auxiliary subunits ($\alpha_2\delta$) of the L-type calcium channels, causes autosomal recessive progressive cone dystrophy.[59] The gene encoding the L-type calcium channel α_1-subunit named *CACNA1F* is associated with other types of retinal dysfunction namely incomplete X-linked congenital stationary night blindness (CSNB2)[60, 61] and X-linked cone-rod dystrophy (CORDX3).[62] The main cellular function of $Ca_v1.4$ (α_{1F}) is thought to be mediation of neurotransmitter release from photoreceptor and bipolar cells,[63] a function that could be assumed for $Ca_v1.3$ (α_{1D}) as well. Therefore, and because of the $Ca_v1.3$ (α_{1D}) expression in the developing retina, *CACNA1D* is a candidate gene for retinal dysfunction in man. However, no mutations have been described in patients with retinal disorders and animal models with defects in *Cacna1d* do not exhibit a retinal phenotype. Despite the absence of an obvious retinal phenotype in a $Ca_v1.3^{-/-}$ mouse model there is a reduced electroretinogram (ERG) light peak (LP) amplitude.[64] The LP of the ERG reflects the depolarization of the basolateral plasma membrane of the retinal pigment epithelium (RPE), resulting from changes in the activity of one or more calcium-sensitive chloride channels.[65] However, we did not observe immunostaining of $Ca_v1.3$ (α_{1D}) in the RPE (Fig. 2B). The

lack of retinal phenotypes in the animal models might be due to compensation by other α-subunits. In zebrafish, $Ca_v1.3b$ is one of the obvious candidates[22] and in mouse this could be $Ca_v1.4$ (α_{1F}).[60-62] The absence of a retinal dysfunction of the $Ca_v1.3^{-/-}$ defective mice does not rule out a retinal dysfunction in humans with defects in the orthologous gene since several mouse mutants with defects in genes involved in Usher syndrome do not exhibit retinal degeneration, but only mild ERG abnormalities in some of these.[65-69] For the whirler mouse with defects in the *Whrn* gene, no retinal phenotype has been reported. However, progressive retinal degeneration has been described for a *Whrn* knock-out mouse (Yang J, et al. *IOVS* 2008;49:ARVO E-Abstract 4405). Whether the $Ca_v1.3$ (α_{1D}) localization or function is disturbed in this mouse mutant remains to be determined. To the authors' knowledge, no locus for syndromic or nonsyndromic retinal dysfunction or deafness has been reported for the *CACNA1D* locus. The locus for Usher syndrome type 2b, which harbored the *CACNA1D* gene, has recently been withdrawn.[70, 71]

References

1. Smith RJ, Berlin CI, Hejtmancik JF, et al. Clinical diagnosis of the Usher syndromes. Usher Syndrome Consortium. *Am J Med Genet*. 1994;50:32-38.
2. Ahmed ZM, Riazuddin S, Riazuddin S, Wilcox ER. The molecular genetics of Usher syndrome. *Clin Genet*. 2003;63:431-444.
3. Ahmed ZM, Riazuddin S, Khan SN, Friedman PL, Riazuddin S, Friedman TB. USH1H, a novel locus for type I Usher syndrome, maps to chromosome 15q22-23. *Clin Genet*. 2009;75:86-91.
4. Chaib H, Kaplan J, Gerber S, et al. A newly identified locus for Usher syndrome type I, USH1E, maps to chromosome 21q21. *Hum Mol Genet*. 1997;6:27-31.
5. Ebermann I, Scholl HP, Charbel IP, et al. A novel gene for Usher syndrome type 2: mutations in the long isoform of whirlin are associated with retinitis pigmentosa and sensorineural hearing loss. *Hum Genet*. 2007;121:203-211.
6. Kremer H, van Wijk E, Marker T, Wolfrum U, Roepman R. Usher syndrome: molecular links of pathogenesis, proteins and pathways. *Hum Mol Genet*. 2006;15 Suppl 2:R262-R270.
7. Petit C. Usher syndrome: from genetics to pathogenesis. *Annu Rev Genomics Hum Genet*. 2001;2:271-297.
8. Reiners J, Nagel-Wolfrum K, Jurgens K, Marker T, Wolfrum U. Molecular basis of human Usher syndrome: deciphering the meshes of the Usher protein network provides insights into the pathomechanisms of the Usher disease. *Exp Eye Res*. 2006;83:97-119.
9. Weil D, El Amraoui A, Masmoudi S, et al. Usher syndrome type I G (USH1G) is caused by mutations in the gene encoding SANS, a protein that associates with the USH1C protein, harmonin. *Hum Mol Genet*. 2003;12:463-471.
10. Weston MD, Luijendijk MW, Humphrey KD, Moller C, Kimberling WJ. Mutations in the VLGR1 gene implicate G-protein signaling in the pathogenesis of Usher syndrome type II. *Am J Hum Genet*. 2004;74:357-366.
11. Rivolta C, Sweklo EA, Berson EL, Dryja TP. Missense mutation in the USH2A gene: association with recessive retinitis pigmentosa without hearing loss. *Am J Hum Genet*. 2000;66:1975-1978.
12. Seyedahmadi BJ, Rivolta C, Keene JA, Berson EL, Dryja TP. Comprehensive screening of the USH2A gene in Usher syndrome type II and non-syndromic recessive retinitis pigmentosa. *Exp Eye Res*. 2004;79:167-173.

13. Adato A, Michel V, Kikkawa Y, et al. Interactions in the network of Usher syndrome type 1 proteins. *Hum Mol Genet*. 2005;14:347-356.
14. Reiners J, van Wijk E, Marker T, et al. Scaffold protein harmonin (USH1C) provides molecular links between Usher syndrome type 1 and type 2. *Hum Mol Genet*. 2005;14:3933-3943.
15. van Wijk E, van der Zwaag B, Peters T, et al. The DFNB31 gene product whirlin connects to the Usher protein network in the cochlea and retina by direct association with USH2A and VLGR1. *Hum Mol Genet*. 2006;15:751-765.
16. Reiners J, Marker T, Jurgens K, Reidel B, Wolfrum U. Photoreceptor expression of the Usher syndrome type 1 protein protocadherin 15 (USH1F) and its interaction with the scaffold protein harmonin (USH1C). *Mol Vis*. 2005;11:347-355.
17. Maerker T, van Wijk E, Overlack N, et al. A novel Usher protein network at the periciliary reloading point between molecular transport machineries in vertebrate photoreceptor cells. *Hum Mol Genet*. 2008;17:71-86.
18. van Wijk E, Kersten FF, Kartono A, et al. Usher syndrome and Leber congenital amaurosis are molecularly linked via a novel isoform of the centrosomal ninein-like protein. *Hum Mol Genet*. 2009;18:51-64.
19. Jelen F, Oleksy A, Smietana K, Otlewski J. PDZ domains - common players in the cell signaling. *Acta Biochim Pol*. 2003;50:985-1017.
20. Bateman A, Coin L, Durbin R, et al. The Pfam protein families database. *Nucleic Acids Res*. 2004;32:D138-D141.
21. Platzer J, Engel J, Schrott-Fischer A, et al. Congenital deafness and sinoatrial node dysfunction in mice lacking class D L-type Ca2+ channels. *Cell*. 2000;102:89-97.
22. Sidi S, Busch-Nentwich E, Friedrich R, Schoenberger U, Nicolson T. gemini encodes a zebrafish L-type calcium channel that localizes at sensory hair cell ribbon synapses. *J Neurosci*. 2004;24:4213-4223.
23. Roepman R, Schick D, Ferreira PA. Isolation of retinal proteins that interact with retinitis pigmentosa GTPase regulator by interaction trap screen in yeast. *Methods Enzymol*. 2000;316:688-704.
24. Trojan P, Krauss N, Choe HW, Giessl A, Pulvermuller A, Wolfrum U. Centrins in retinal photoreceptor cells: regulators in the connecting cilium. *Prog Retin Eye Res*. 2008;27:237-259.
25. Gherman A, Davis EE, Katsanis N. The ciliary proteome database: an integrated community resource for the genetic and functional dissection of cilia. *Nat Genet*. 2006;38:961-962.
26. Williams DS. Usher syndrome: animal models, retinal function of Usher proteins, and prospects for gene therapy. *Vision Res*. 2008;48:433-441.
27. Dolphin AC. Calcium channel diversity: multiple roles of calcium channel subunits. *Curr Opin Neurobiol*. 2009.
28. Arikkath J, Campbell KP. Auxiliary subunits: essential components of the voltage-gated calcium channel complex. *Curr Opin Neurobiol*. 2003;13:298-307.
29. Catterall WA. Structure and regulation of voltage-gated Ca2+ channels. *Annu Rev Cell Dev Biol*. 2000;16:521-555.
30. Song H, Nie L, Rodriguez-Contreras A, Sheng ZH, Yamoah EN. Functional interaction of auxiliary subunits and synaptic proteins with Ca(v)1.3 may impart hair cell Ca2+ current properties. *J Neurophysiol*. 2003;89:1143-1149.
31. Dou H, Vazquez AE, Namkung Y, et al. Null mutation of alpha1D Ca2+ channel gene results in deafness but no vestibular defect in mice. *J Assoc Res Otolaryngol*. 2004;5:215-226.
32. Kamphuis W, Hendriksen H. Expression patterns of voltage-dependent calcium channel alpha 1 subunits (alpha 1A-alpha 1E) mRNA in rat retina. *Brain Res Mol Brain Res*. 1998;55:209-220.
33. Xiao H, Chen X, Steele EC, Jr. Abundant L-type calcium channel Ca(v)1.3 (alpha1D) subunit mRNA is detected in rod photoreceptors of the mouse retina via in situ hybridization. *Mol Vis*. 2007;13:764-771.
34. Xu HP, Zhao JW, Yang XL. Expression of voltage-dependent calcium channel subunits in the rat retina. *Neurosci Lett*. 2002;329:297-300.
35. Henderson D, Doerr TA, Gottesman J, Miller RF. Calcium channel immunoreactivity in the salamander retina. *Neuroreport*. 2001;12:1493-1499.
36. Welch NC, Wood S, Jollimore C, Stevens K, Kelly ME, Barnes S. High-voltage-activated calcium channels in Muller cells acutely isolated from tiger salamander retina. *Glia*. 2005;49:259-274.

37. Knirsch M, Brandt N, Braig C, et al. Persistence of Ca(v)1.3 Ca2+ channels in mature outer hair cells supports outer hair cell afferent signaling. *J Neurosci*. 2007;27:6442-6451.
38. Yap CC, Liang F, Yamazaki Y, et al. CIP98, a novel PDZ domain protein, is expressed in the central nervous system and interacts with calmodulin-dependent serine kinase. *J Neurochem*. 2003;85:123-134.
39. Aartsen WM, Kantardzhieva A, Klooster J, et al. Mpp4 recruits Psd95 and Veli3 towards the photoreceptor synapse. *Hum Mol Genet*. 2006;15:1291-1302.
40. Morgans CW, Bayley PR, Oesch NW, Ren G, Akileswaran L, Taylor WR. Photoreceptor calcium channels: insight from night blindness. *Vis Neurosci*. 2005;22:561-568.
41. Brandt A, Striessnig J, Moser T. CaV1.3 channels are essential for development and presynaptic activity of cochlear inner hair cells. *J Neurosci*. 2003;23:10832-10840.
42. Brandt A, Khimich D, Moser T. Few CaV1.3 channels regulate the exocytosis of a synaptic vesicle at the hair cell ribbon synapse. *J Neurosci*. 2005;25:11577-11585.
43. Hafidi A, Dulon D. Developmental expression of Ca(v)1.3 (alpha1d) calcium channels in the mouse inner ear. *Brain Res Dev Brain Res*. 2004;150:167-175.
44. Papermaster DS, Schneider BG, DeFoe D, Besharse JC. Biosynthesis and vectorial transport of opsin on vesicles in retinal rod photoreceptors. *J Histochem Cytochem*. 1986;34:5-16.
45. Roepman R, Wolfrum U. Protein networks and complexes in photoreceptor cilia. *Subcell Biochem*. 2007;43:209-235.
46. Deretic D, Papermaster DS. Polarized sorting of rhodopsin on post-Golgi membranes in frog retinal photoreceptor cells. *J Cell Biol*. 1991;113:1281-1293.
47. Mazelova J, Ransom N, stuto-Gribble L, Wilson MC, Deretic D. Syntaxin 3 and SNAP-25 pairing, regulated by omega-3 docosahexaenoic acid, controls the delivery of rhodopsin for the biogenesis of cilia-derived sensory organelles, the rod outer segments. *J Cell Sci*. 2009;122:2003-2013.
48. Hibino H, Pironkova R, Onwumere O, Vologodskaia M, Hudspeth AJ, Lesage F. RIM binding proteins (RBPs) couple Rab3-interacting molecules (RIMs) to voltage-gated Ca(2+) channels. *Neuron*. 2002;34:411-423.
49. Ramakrishnan NA, Drescher MJ, Drescher DG. Direct interaction of otoferlin with syntaxin 1A, SNAP-25, and the L-type voltage-gated calcium channel Cav1.3. *J Biol Chem*. 2009;284:1364-1372.
50. Lin RC, Scheller RH. Mechanisms of synaptic vesicle exocytosis. *Annu Rev Cell Dev Biol*. 2000;16:19-49.
51. Safieddine S, Wenthold RJ. SNARE complex at the ribbon synapses of cochlear hair cells: analysis of synaptic vesicle- and synaptic membrane-associated proteins. *Eur J Neurosci*. 1999;11:803-812.
52. Kachar B, Battaglia A, Fex J. Compartmentalized vesicular traffic around the hair cell cuticular plate. *Hear Res*. 1997;107:102-112.
53. Chuang JZ, Zhao Y, Sung CH. SARA-regulated vesicular targeting underlies formation of the light-sensing organelle in mammalian rods. *Cell*. 2007;130:535-547.
54. Kwok MC, Holopainen JM, Molday LL, Foster LJ, Molday RS. Proteomics of photoreceptor outer segments identifies a subset of SNARE and Rab proteins implicated in membrane vesicle trafficking and fusion. *Mol Cell Proteomics*. 2008;7:1053-1066.
55. Boesze-Battaglia K, Albert AD, Yeagle PL. Fusion between disk membranes and plasma membrane of bovine photoreceptor cells is calcium dependent. *Biochemistry*. 1992;31:3733-3738.
56. Jena BP. Membrane fusion: role of SNAREs and calcium. *Protein Pept Lett*. 2009;16:712-717.
57. Leabu M. Membrane fusion in cells: molecular machinery and mechanisms. *J Cell Mol Med*. 2006;10:423-427.
58. Baumann L, Gerstner A, Zong X, Biel M, Wahl-Schott C. Functional characterization of the L-type Ca2+ channel Cav1.4alpha1 from mouse retina. *Invest Ophthalmol Vis Sci*. 2004;45:708-713.
59. Wycisk KA, Zeitz C, Feil S, et al. Mutation in the auxiliary calcium-channel subunit CACNA2D4 causes autosomal recessive cone dystrophy. *Am J Hum Genet*. 2006;79:973-977.
60. Bech-Hansen NT, Naylor MJ, Maybaum TA, et al. Loss-of-function mutations in a calcium-channel alpha1-subunit gene in Xp11.23 cause incomplete X-linked congenital stationary night blindness. *Nat Genet*. 1998;19:264-267.
61. Strom TM, Nyakatura G, pfelstedt-Sylla E, et al. An L-type calcium-channel gene mutated in incomplete X-linked congenital stationary night blindness. *Nat Genet*. 1998;19:260-263.

62. Jalkanen R, Mantyjarvi M, Tobias R, et al. X linked cone-rod dystrophy, CORDX3, is caused by a mutation in the CACNA1F gene. *J Med Genet*. 2006;43:699-704.
63. Berntson A, Taylor WR, Morgans CW. Molecular identity, synaptic localization, and physiology of calcium channels in retinal bipolar cells. *J Neurosci Res*. 2003;71:146-151.
64. Wu J, Marmorstein AD, Striessnig J, Peachey NS. Voltage-dependent calcium channel CaV1.3 subunits regulate the light peak of the electroretinogram. *J Neurophysiol*. 2007;97:3731-3735.
65. Gallemore RP, Steinberg RH. Light-evoked modulation of basolateral membrane Cl- conductance in chick retinal pigment epithelium: the light peak and fast oscillation. *J Neurophysiol*. 1993;70:1669-1680.
66. Haywood-Watson RJ, Ahmed ZM, Kjellstrom S, et al. Ames Waltzer deaf mice have reduced electroretinogram amplitudes and complex alternative splicing of Pcdh15 transcripts. *Invest Ophthalmol Vis Sci*. 2006;47:3074-3084.
67. Libby RT, Steel KP. Electroretinographic anomalies in mice with mutations in Myo7a, the gene involved in human Usher syndrome type 1B. *Invest Ophthalmol Vis Sci*. 2001;42:770-778.
68. Libby RT, Kitamoto J, Holme RH, Williams DS, Steel KP. Cdh23 mutations in the mouse are associated with retinal dysfunction but not retinal degeneration. *Exp Eye Res*. 2003;77:731-739.
69. McGee J, Goodyear RJ, McMillan DR, et al. The very large G-protein-coupled receptor VLGR1: a component of the ankle link complex required for the normal development of auditory hair bundles. *J Neurosci*. 2006;26:6543-6553.
70. Hmani-Aifa M, Benzina Z, Zulfiqar F, et al. Identification of two new mutations in the GPR98 and the PDE6B genes segregating in a Tunisian family. *Eur J Hum Genet*. 2008.
71. Hmani M, Ghorbel A, Boulila-Elgaied A, et al. A novel locus for Usher syndrome type II, USH2B, maps to chromosome 3 at p23-24.2. *Eur J Hum Genet*. 1999;7:363-367.

FIGURE LEGENDS

Figure 1. Validation of $Ca_v1.3$ (α_{1D}) - whirlin interaction. **(A)** Yeast two-hybrid assays were performed with a part of the $Ca_v1.3$ (α_{1D}) C-terminus fused to the activation domain (AD) and whirlin PDZ1, PDZ2, PDZ1+2 and PDZ3 or harmonin PDZ1, PDZ2 and PDZ3 fused to the DNA binding domain (BD) of the GAL4 reporter gene, respectively. $Ca_v1.3$ (α_{1D}) interacts with the PDZ1 and/or PDZ2 domains, but not with the PDZ3 domain of whirlin. $Ca_v1.3$ (α_{1D}) interacts with the PDZ1 and PDZ3, but not with the PDZ2 domain of harmonin, but this interaction was weak (+) as compared to the $Ca_v1.3$ (α_{1D}) – whirlin (++) interaction. **(B)** GST pull-down assays showing that HA-tagged whirlin was efficiently pulled down by GST- $Ca_v1.3$ (α_{1D}) C-terminus, but not by $Ca_v1.3$ (α_{1D})ΔPBM or GST alone, as detected by an anti-whirlin antibody. The first lane shows 2% of the input of COS-1 cell lysate. **(C)** GST pull-down assays, showing that eCFP-tagged $Ca_v1.3$ (α_{1D}), detected by an anti-GFP antibody, was efficiently pulled down by GST- whirlin PDZ1, PDZ2 and PDZ1+2, but not by GST-whirlin PDZ3 or GST alone. The first lane shows 1.5% of the input eCFP- $Ca_v1.3$ (α_{1D}) protein lysate. **(D)** Co-immunoprecipitation assay from COS-1 cell lysates, showing that eCFP-whirlin co-immunoprecipitated with the HA-tagged C-terminal region of $Ca_v1.3$ (α_{1D}), but not with the HA-tagged protein Plk1. **(E)**

GST pull-down assay, showing that HA-tagged harmonin not was pulled down by GST- $Ca_v1.3$ (α_{1D}) C-terminus with the PBM or GST alone, as detected by an anti-HA antibody. The first lane shows 2% of the input of COS-1 cell lysate.

Figure 2. Whirlin and $Ca_v1.3$ (α_{1D}) co-localize in rat photoreceptor cells. Subcellular localization of whirlin and $Ca_v1.3$ (α_{1D}) in retina cryosections of adult (P20) rat. **(A-C)** Immunostaining respectively with anti-whirlin (green), anti-$Ca_v1.3$ (α_{1D}) (red) and an overlay (yellow) indicates co-localization at the region of the connecting cilium (CC; open arrow heads), the outer limiting membrane (OLM; closed arrow heads) and the outer plexiform layer (OPL). **(D-F)** Immunofluorescence with anti-$Ca_v1.3$ (α_{1D}) (green) and anti-*pan* centrin (red) as a marker for the connecting cilium, centriole and basal body confirmed the localization in this region since partial co-localization (yellow) was observed.

Figure 3. Localization of $Ca_v1.3$ (α_{1D}) by immunoelectron microscopy. Electron micrographs of anti-$Ca_v1.3$ (α_{1D}) labelling in longitudinal **(A-C, E-F)** and cross **(D)** sections of rod mouse photoreceptor cells. $Ca_v1.3$ (α_{1D}) was detected in the collar-like extension of the apical inner segment (CE) **(A-B)**, at the basal body complex (BB) **(B-C)** and in the connecting cilium (CC) **(B-D)**. $Ca_v1.3$ (α_{1D}) was also detected in the base of the outer segment (OS) **(A-C)** and at the synapses (S) of mouse photoreceptor **(E-F)**. Inner segment (IS) Scale bars: A-C: 0.25 µm, D,F: 0.1 µm, E: 0.5 µm.

Figure 4. RNA *In situ* hybridization of *Cacna1d* mRNA in embryonic and adult mouse**.** *Cacna1d* was widely expressed during development (E12.5-E16.5), with most intense signals, in the following structures (indicated by numbers and arrow heads). **(A)** neopallial cortex (1), midbrain (2), lung (3), adrenal gland (4), spinal cord (5), stomach wall (6), tongue (7), olfactory epithelium (8). Expression was also observed in the kidney, choroid plexus of the fourth ventricle, the lower and upper jaws, olfactory bulb, trigeminal (V) ganglion, duodenum, thalamus, umbilical cord, and venous heart region (data not shown). **(B-H)** A strong signal for *Cacna1d* was observed in the eye. Embryonic development of the eye at E12.5 (B) and E14.5 (C), in which expression was observed in the whole neuroblastic layer of the retina. At E16.5 (D), *Cacna1d* was expressed in the inner neuroblastic layer of the retina, and at E18.5 (E) expression was observed in a subset of the cells and the inner nuclear

layer (INL). Expression of *Cacna1d* was maintained at postnatal day 7 (F) and 90 (G-H). A strong signal, indicative of a high level of expression, was observed in the inner nuclear layer (INL) and a subset of the ganglion cells (GCL). Furthermore, expression was seen in the outer nuclear layer (ONL) and inner segments (IS) (H). **(I-J, L-O)** From E14.5 onwards, *Cacna1d* expression in the developing inner ear was observed and became more pronounced at E16.5 (I-J, L-O). Sections of the developing inner ear at E16.5 with *Cacna1d* expression in the inner hair cell (L-M, 1), the spiral ganglion cells (M, 2), developing sensory cells of the macula of the utricle (N, 3), and in the crista ampullaris of the semicircular canals (O, 4). To increase structural detail, a number of sections were counterstained with Nuclear Fast Red (L-O). **(K)** Sections hybridized with the sense *Cacna1d* cRNA probe revealed no staining, indicating the specificity of antisense cRNA probe used in these experiments.

A

	pAD $Ca_v1.3$
pBD whirlin PDZ 1	++
pBD whirlin PDZ 2	++
pBD whirlin PDZ 1+2	++
pBD whirlin PDZ 3	-
pBD harmonin PDZ 1	+
pBD harmonin PDZ 2	-
pBD harmonin PDZ 3	+

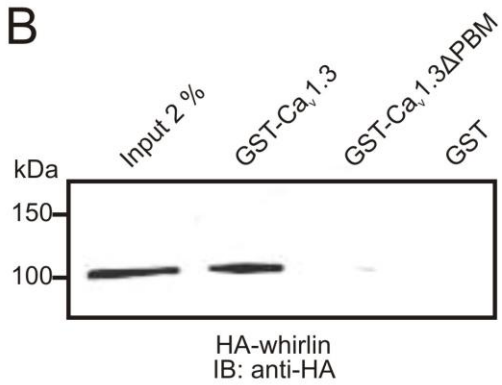

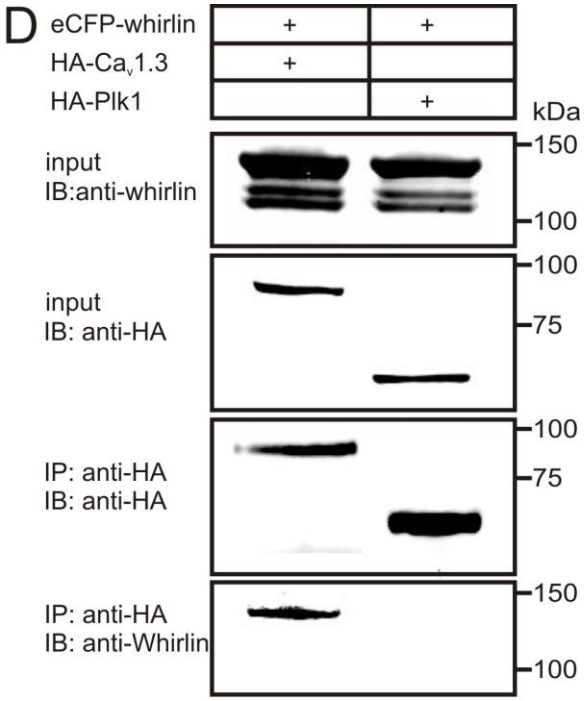

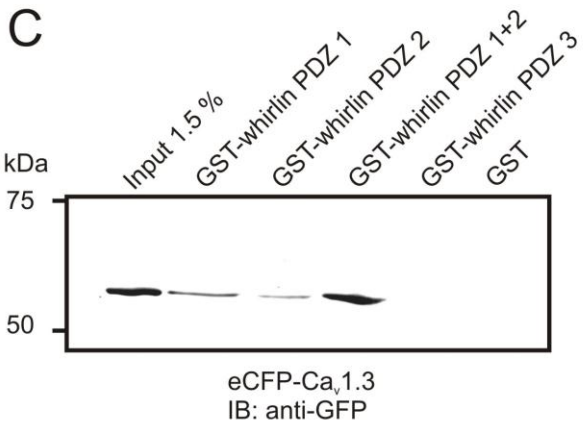

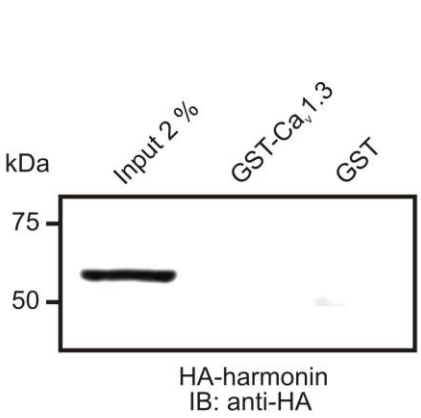

Figure 1

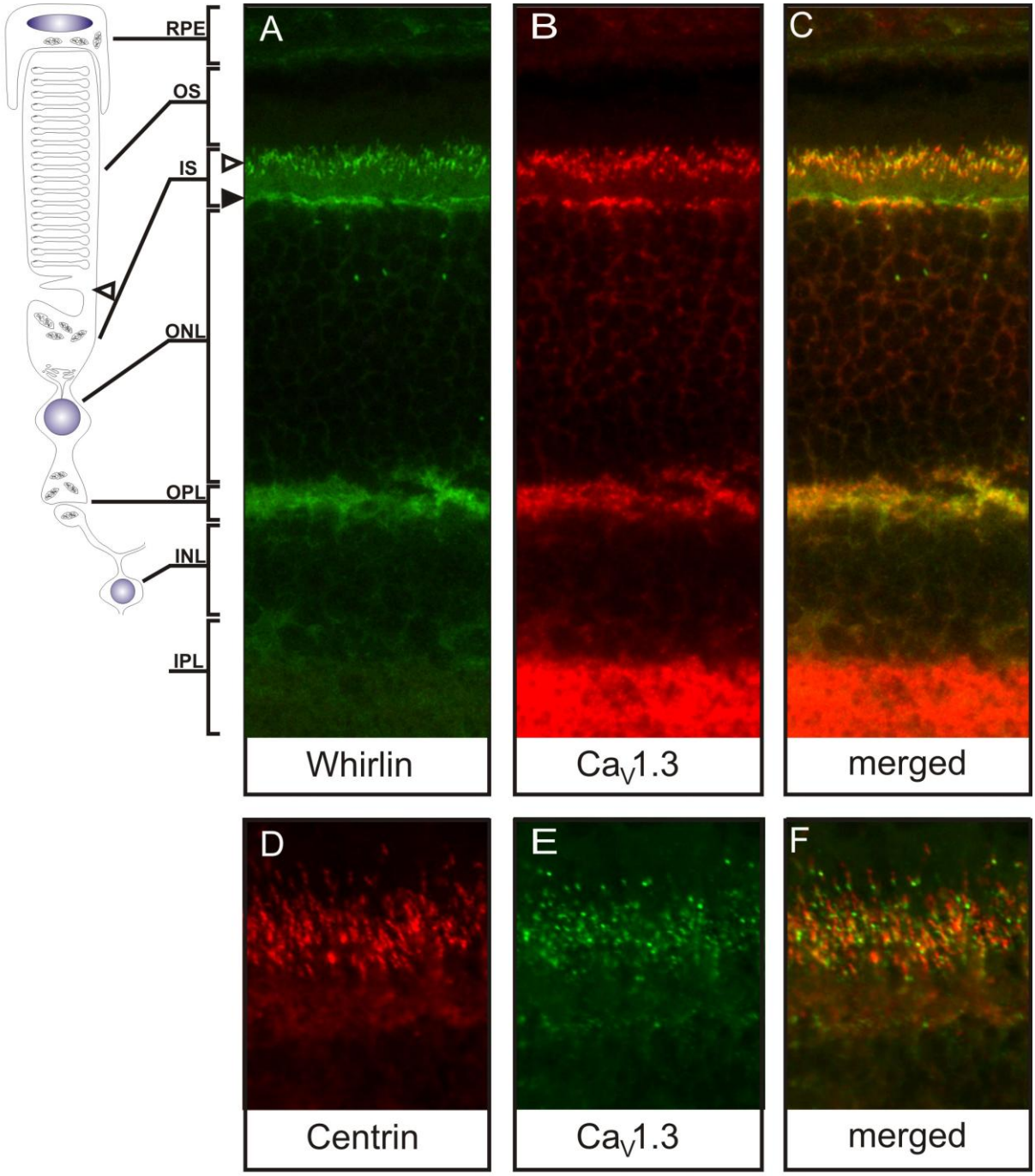
RPE
OS
IS
ONL
OPL
INL
IPL
A
B
C
Whirlin
$Ca_V1.3$
merged
D
E
F
Centrin
$Ca_V1.3$
merged

Figure 2

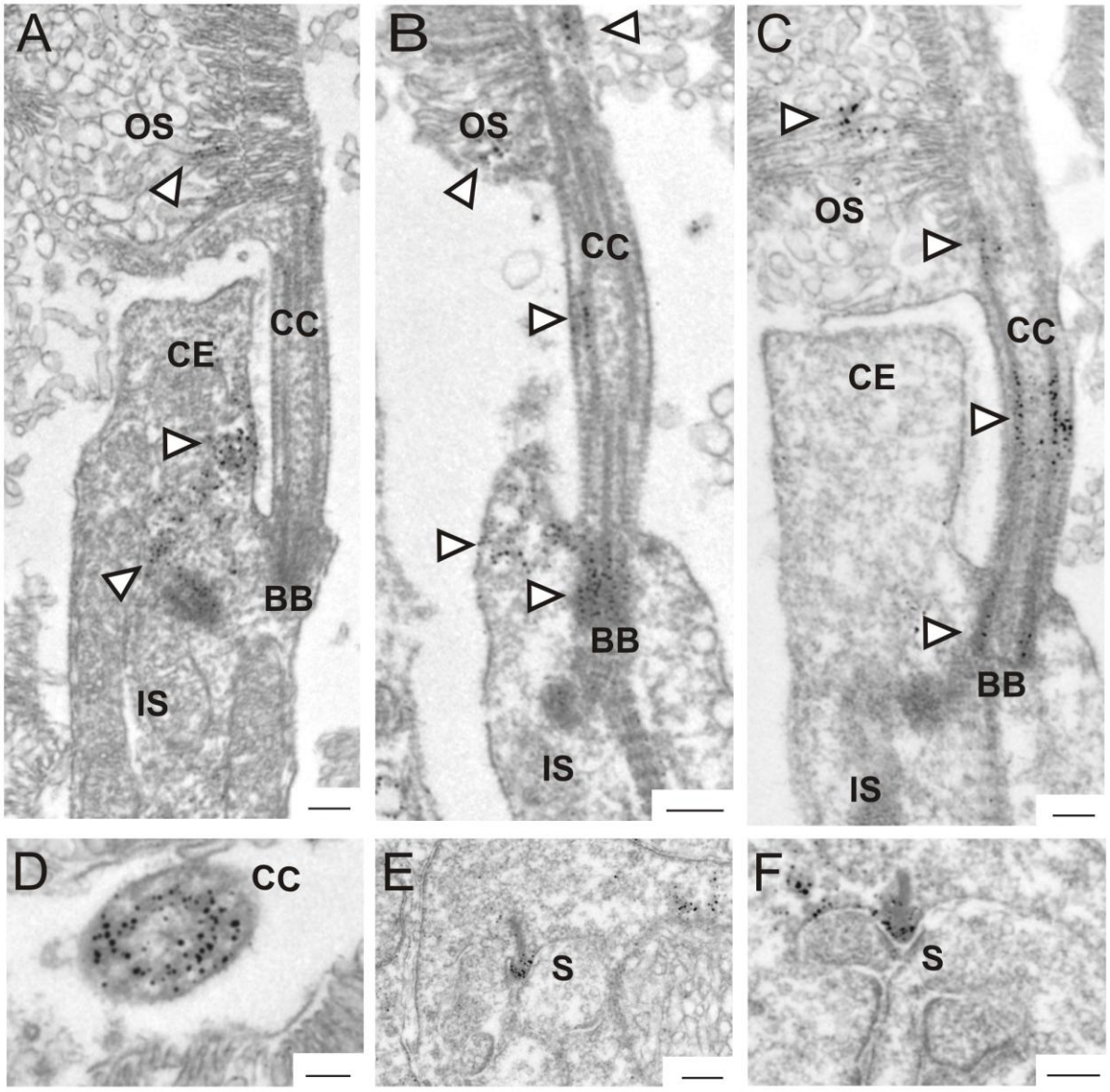

Figure 3

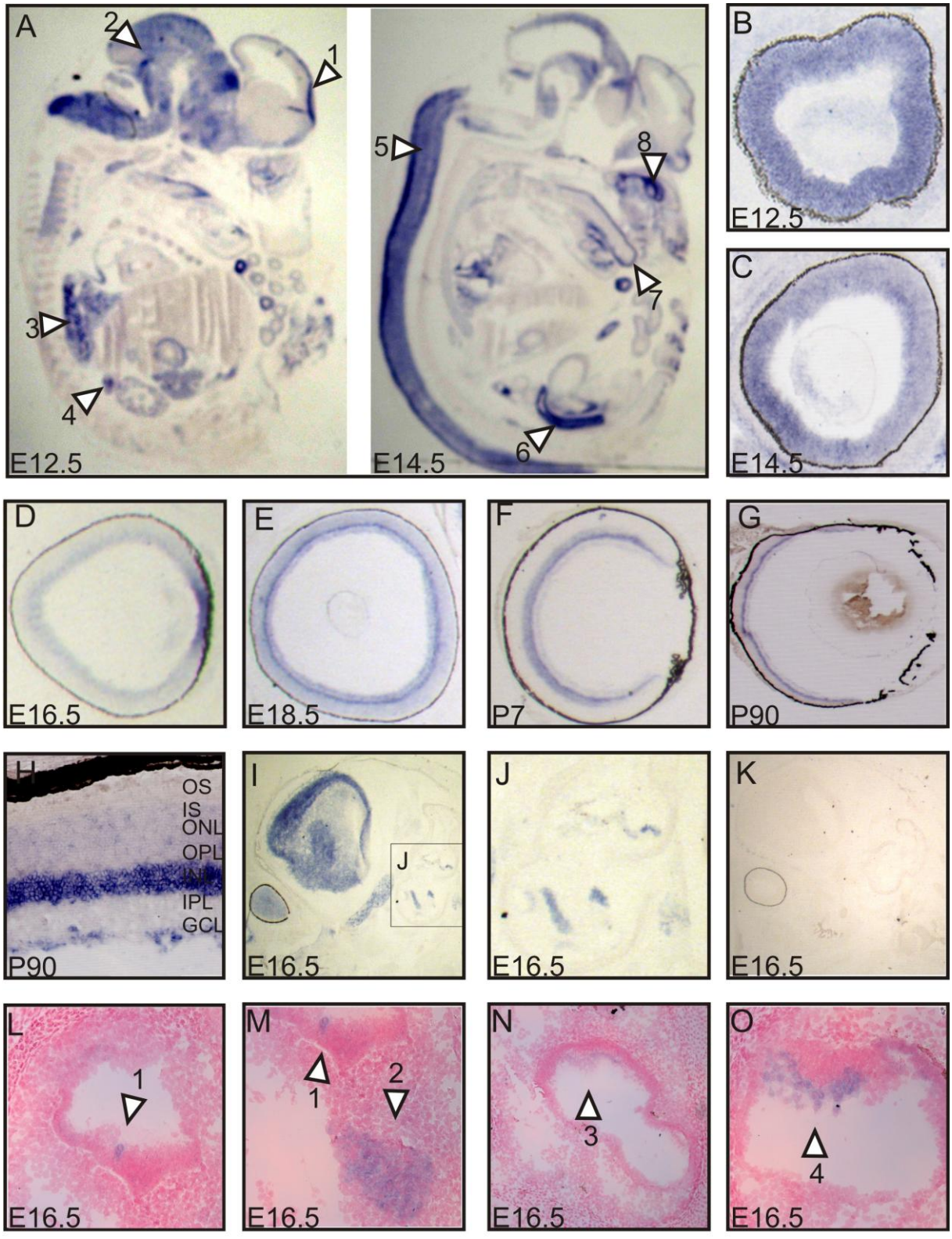
A
2
1
3
4
E12.5
5
8
7
6
E14.5
B
E12.5
C
E14.5
D
E16.5
E
E18.5
F
P7
G
P90
H
OS
IS
ONL
OPL
INL
IPL
GCL
P90
I
J
E16.5
J
E16.5
K
E16.5
L
1
E16.5
M
1
2
E16.5
N
3
E16.5
O
4
E16.5

Figure 4